Binary PAH-mixtures cause additive or antagonistic effects on gene expression but synergistic effects on DNA adduct formation.

Carcinogenesis vol.28 no.12 pp.2632–2640, 2007
doi:10.1093/carcin/bgm182
Advance Access publication August 8, 2007

Binary PAH mixtures cause additive or antagonistic effects on gene expression but synergistic effects on DNA adduct formation

Yvonne C.M.Staal[1,2], Dennie G.A.J.Hebels[1], Marcel H.M.van Herwijnen[1], Ralph W.H.Gottschalk[1], Frederik J.van Schooten and Joost H.M.van Delft[1,*]

[1]Department of Health Risk Analysis and Toxicology, Maastricht University, PO Box 616, 6200 MD Maastricht, The Netherlands

[2]Present address: TNO Quality of Life, Department of Toxicology and Applied Pharmacology, PO box 360, 3700 AJ Zeist, The Netherlands

[*]To whom correspondence should be addressed. Tel: +31 43 388 1092; Fax: +31 43 388 4146;
Email: j.vandelft@grat.unimaas.nl

Polycyclic aromatic hydrocarbons (PAHs) cover a wide range of structurally related compounds which differ greatly in their carcinogenic potency. PAH exposure usually occurs through mixtures rather than individual compounds. Therefore, we assessed whether the effects of binary PAH mixtures on gene expression, DNA adduct formation, apoptosis and cell cycle are additive compared with the effects of the individual compounds in human hepatoma cells (HepG2). Equimolar and equitoxic mixtures of benzo[*a*]pyrene (B[*a*]P) with either dibenzo[a,l]pyrene (DB[a,l]P), dibenzo[a,h]anthracene (DB[a,h]A), benzo[b]fluoranthene (B[b]F), fluoranthene (FA) or 1-methylphenanthrene (1-MPA) were studied. DB[a,l]P, B[*a*]P, DB[a,h]A and B[b]F dose-dependently increased apoptosis and blocked cells cycle in S-phase. PAH mixtures showed an additive effect on apoptosis and on cell cycle blockage. DNA adduct formation in mixtures was higher than expected based on the individual compounds, indicating a synergistic effect of PAH mixtures. Equimolar mixtures of B[*a*]P and DB[a,l]P (0.1, 0.3 and 1.0 μM) were assessed for their effects on gene expression. Only at 1.0 μM, the mixture showed antagonism. All five compounds were also tested as a binary mixture with B[*a*]P in equitoxic concentrations. The combinations of B[*a*]P with B[b]F, DB[a,h]A or FA showed additivity, whereas B[*a*]P with DB[a,l]P or 1-MPA showed antagonism. Many individual genes showed additivity in mixtures, but some genes showed mostly antagonism or synergism. Our results show that the effects of binary mixtures of PAHs on gene expression are generally additive or slightly antagonistic, suggesting no effect or decreased carcinogenic potency, whereas the effects on DNA adduct formation show synergism, which rather indicates increased carcinogenic potency.

Introduction

Polycyclic aromatic hydrocarbons (PAHs) are organic compounds present in the air after incomplete combustion of organic fuels. PAHs cover a wide range of structurally related compounds with a diverse range in carcinogenic and mutagenic potency.

Many PAHs bind to the Aryl hydrocarbon (Ah) receptor, which translocates to the nucleus and induces the expression of several genes, among which several genes for cytochrome P450 enzymes (e.g. *CYP1A1*, *CYP1A2* and *CYP1B1*) (1). These enzymes are capable of metabolizing PAHs to their reactive intermediates (2). PAHs vary in their affinity for the Ah-receptor and thereby the induction of cytochrome P450 enzymes will vary accordingly (3). Many PAHs are able to bind to DNA after metabolic activation and thereby form DNA adducts. When these DNA adducts are not properly removed or repaired, mutations can occur and thereby induction of cancer development (4). Although different PAH adducts are repaired with different accuracy and at different rate, DNA adduct formation has been shown to correlate with mutagenic potency of PAHs (4,5). DNA adducts can also affect the p53 pathway, which may lead to changes in biological processes (such as cell cycle arrest or apoptosis) (6). We have shown previously that PAHs can induce compound-specific gene expression profiles in HepG2 cells and that these profiles can be related to the carcinogenic potency of the PAH (7).

PAH exposure usually occurs through mixtures, and the various compounds may modulate the effect of other compounds. PAH interactions can lead to an addition of the effect of both PAHs (additivity) or to a higher effect than expected based on additivity (synergism), or PAHs may repress the effects of the other PAH (antagonism) (8,9). Either synergism or antagonism can be expected in PAH mixtures, which is further explained by two hypotheses.

The first hypothesis suggests synergism, which occurs when the metabolism of a compound is influenced by another (10). This may occur, for example, when cells are exposed to benzo[*a*]pyrene (B[*a*]P)—an inducer of the *CYP1A1* gene expression—in combination with a PAH which is not able to induce *CYP1A1*. The non-*CYP1A1* inducing compound may be metabolically activated at increased rate by the B[*a*]P-induced *CYP1A1* levels, thereby leading to enhanced DNA adduct formation and consequently enhanced mutagenesis and carcinogenesis.

The second hypothesis suggests antagonism. It has been shown that the expression of the *CYP1A1* gene and protein is decreased in HepG2 cells after exposure to B[*a*]P and 1-nitropyrene compared with B[*a*]P alone (11). This was also found for mixtures of B[*a*]P with fluoranthene (FA) in the EROD assay (12). Theoretically, this would lead to decreased metabolism of B[*a*]P and thereby less DNA adduct formation and reduced toxic and carcinogenic potency of B[*a*]P.

This study aims to gain knowledge on interactive effects in binary PAH mixtures on gene expression profiles in human cells. To our knowledge, we are the first to study the effects of binary PAH mixtures on gene expression profiles obtained by microarray technology, combined with apoptosis, cell cycle and DNA adduct formation.

Since liver is an important organ in metabolism of xenobiotic compounds, and the human hepatoma cell line HepG2 is competent in PAH metabolism and was shown to give PAH-specific gene expression profiles, we used this cell line to study interaction between PAHs. Six PAHs were selected based on their environmental occurrence and carcinogenic potency (13,14), namely in order of occurrence benzo[b]fluoranthene (B[b]F) ≈ fluoranthene (FA) ≈ 1-methylphenanthrene (1-MPA) > B[*a*]P > dibenzo[a,h]anthracene (DB[a,h]A) > dibenzo[a,l]pyrene (DB[a,l]P). Carcinogenic potency differs greatly between these PAHs and can be arranged from high to low: DB[a,l]P > DB[a,h]A > B[*a*]P > Bb]F > FA ≈ 1-MPA. B[*a*]P, B[b]F and DB[a,h]A induced the *CYP1A1* expression, whereas DB[a,l]P mildly induced *CYP1A1* and FA and 1-MPA did not affect the expression of *CYP1A1* (7). We assessed the effects of equimolar mixtures of B[*a*]P and DB[a,l]P in the low toxic range as well as the effects of equitoxic mixtures of each PAH with B[*a*]P. We measured cell cycle distribution and apoptosis by FACS analysis, DNA adduct formation by ^{32}P-post-labelling and gene expression changes by microarray analysis using a PHASE-I array containing 600 toxicologically relevant genes. All data were used to study the effects of a mixture of PAH in relation to the effects of the individual compounds using an additive model to estimate the mixture effect.

Abbreviations: B[*a*]P, benzo[*a*]pyrene; B[b]F, benzo[b]fluoranthene; DB[a,h]A, dibenzo[a,h]anthracene; DB[a,l]P, dibenzo[a,l]pyrene; DMSO, dimethyl sulfoxide; FA, fluoranthene; PAH, polycyclic aromatic hydrocarbon; PCR, polymerase chain reaction; RT, real-time; 1-MPA, 1-methylphenanthrene.

Materials and methods

Chemicals

B[*a*]P (purity 97%, CAS no. 50-32-8), B[b]F (purity 98%, CAS no. 205-99-2), FA (purity 99%, CAS no. 206-44-0), DB[a,h]A (purity 97%, CAS no. 53-70-3)

and DB[a,l]P (purity 99,6%, CAS no. 191-30-0) were obtained from Sigma-Aldich (Zwijndrecht, The Netherlands). 1-MPA (purity 99%, CAS no. 832-69-9) was obtained from LGC Promchem (Teddington, UK). All chemicals were dissolved in dimethyl sulfoxide (DMSO).

Cell culture and treatment

HepG2 cells were cultured in Minimal Essential Medium supplemented with 1% non-essential amino acids, 1% sodium pyruvate, 2% penicillin/streptomycin and 10% fetal bovine serum (all from Gibco BRL, Breda, The Netherlands) in T25 culture flasks at 37°C and 5% CO_2. One day before treatment, cell cultures at 70–80% confluency were harvested and cells were undiluted divided among six-well plates (for flow cytometry, 600 000 cells) or new culture flasks (for gene expression and DNA adduct analysis, $\sim 2.5 \times 10^6$ cells), in order to obtain a homogeneous cell population for each treatment. The next day, the medium was replaced with fresh medium containing 1 nM to 30 μM of a PAH, an equimolar or equitoxic mixture of two PAHs or a vehicle control (DMSO, 0.1%). The cells were exposed for 24 h, and thereafter either cells were fixed with 2 ml cold methanol and stored at −20°C (six-well plates, for FACS analysis) or media was removed from the culture flasks (∼90% confluent) and 1 ml Trizol (Gibco BRL) was immediately added to the cells (for RNA and DNA isolation). Two independent experiments were conducted.

Flow cytometric analysis for cell cycle and apoptosis

For flow cytometry, we used the primary antibody M30 CytoDeath (Roche, Penzberg, Germany) and the producers' manual. Wash buffer was replaced with phosphate-buffered saline containing 1 mg/ml bovine serum albumin. The secondary antibody, fluorescein isothiocyanate-conjugated anti-mouse Ig, was obtained from DakoCytomation (Glostrup, Denmark), which was incubated in the dark overnight at 4°C. After washing, the cells were re-suspended in 0.5 ml phosphate-buffered saline containing 20 μg/ml propidium iodide and incubated 15 min at room temperature prior to flow cytometric analysis.

A FACSort (Becton Dickinson, Sunnyvale, CA) equipped with an Argon ion laser and a diode laser was used for flow cytometric analysis. An excitation wavelength of 488 nm and emission filters of 515–545 nm band pass and 600 nm low pass were used. For each sample 10 000 cells were analyzed. Fluorescein isothiocyanate signals were recorded as logarithmic amplified data and the propidium iodide signals as linear amplified data. Electronic compensation was used to eliminate any bleed trough of fluorescence. Data analysis was done using CellQuest software (version 3.1, Becton Dickinson, San Jose, CA). Data were gated on pulse-processed propidium iodide signals to exclude doublets and larger aggregates from the analysis.

M30 CytoDeath positive (apoptotic) and negative (non-apoptotic) signals were sorted in the gated population and displayed as percentage of total cells with WinMDI 2.8 (http://facs.scripps.edu/software.html, 15 May 2006). Cell cycle was analyzed on the gated population of single using ModFit LT for Mac (version 2.0). Cells in the G_{0-1}, S or G_2-M phase were expressed as a percentage of the total number of cells.

Expected apoptosis levels were calculated by adding the total percentage of apoptosis of both constituents and subtracting the basal percentage of apoptosis found for the control sample.

DNA adduct formation

As DNA recoveries from cells exposed to equimolar concentrations of PAHs were limited, we only measured DNA adduct formation in cells exposed to equitoxic concentrations of PAHs.

After removal of the aqueous phase during RNA isolation using Trizol (see RNA isolation and quality control), the remaining phases were used for DNA isolation according to manufacturer's protocol. DNA adduct levels were determined according to the procedure originally described by Reddy *et al.* (15) with modifications described by Godschalk *et al.* (16). By including samples with known DNA adduct levels (1 adduct per 10^6, 10^7 or 10^8 nucleotides), DNA adduct levels were quantified (detection limit 1 adduct 10^8 nucleotides).

Adduct spots on the chromatograms were located and quantified using a phosphor imager (FLA-3000, Fuji, Paris, France) and AIDA/2D densometry software.

Expected DNA adduct levels were calculated by adding the total DNA adduct levels of both constituents and subtracting the background DNA adduct level found for the control sample. The limited number of analysis did not allow statistical analysis.

RNA isolation and quality control

RNA was isolated from the Trizol solutions according to the producer's manual and purified with the RNeasy mini kit (Qiagen Westburg bv., Leusden, The Netherlands). RNA quantity was measured on a spectrophotometer and quality was determined on a BioAnalyzer (Agilent Technologies, Breda, The Netherlands). Only RNA samples which showed clear 18S and 28S peaks and with a RNA integrity number level >8 were used for labeling and hybridization.

Gene expression analysis

cDNA synthesis RNA (10 μg per sample) was reverse transcribed into cDNA with amino allyl-labelled deoxyuridine triphosphate (Sigma-Aldrich, St Louis, MO) and subsequently labelled with one of the four dyes, namely Cy3, Cy5, Alexa 488 and Alexa 594. Four instead of two dyes were applied, in order to reduce the variation (four related samples are on one array instead of two) and the number of arrays [as described by Staal *et al.* (17)].

Microarray hybridizations Targets were hybridized on the Human-600 Microarray (PHASE-1 Molecular Toxicology, Santa Fe, NM), containing 597 sequence-verified cDNA clones from human genes, representing a number of toxicologically relevant, as well as control, genes, each printed in quadruplicate. Hybridization and washing was done according to the producers' manual as described previously (17). Hybridization of the equimolar experiment was designed such that all treatments of the same concentration were hybridized on a single array and the dyes were swapped for the technical duplicate. The hybridization design for the equitoxic experiment is shown in supplementary Table 1 (available at Carcinogenesis Online).

Microarray data analysis and data mining The microarray slides were scanned on a ScanArrayExpress (Perkin Elmer life sciences, Boston, MA). All four channels were scanned at 100% laser power and adjusted photo multiplier tube gain, such that the signal of the highest fluorescent spots is just below the maximum measurable level. The images (10 μ resolution; 16 bit tiff) were processed with ImaGene 5.5 software (Biodiscovery, Los Angeles, CA) to quantify spot signals. Abnormal spots were manually or automatically flagged and not included in the data analysis.

Data from ImaGene were transported to GeneSight software version 4.1.6 (Biodiscovery) for transformations, normalizations and analyses. For each spot, background mean was subtracted from signal means; flagged spots and spots with a net expression level <20 were omitted. Data were log base 2 transformed and expression difference between exposed and control were calculated. Data normalization was done by LOWESS. Data of replicate spots were combined while omitting outliers (>2 SDs). Samples from each biological replicate were hybridized twice, thereby providing four hybridizations per PAH concentration (two technical replicates for each biological replicate). Only for B[*a*]P-exposed cells from the equitoxic experiment, eight hybridizations were available (four technical and two biological). Significantly modulated genes were found by the confidence analysis tool in GeneSight, with a minimal up-regulation or down-regulation of 0.5 (after ^{2}log transformation) and a confidence limit of 99%. To obtain equal statistical power for B[*a*]P-exposed cells from the equitoxic experiment, the samples were split into two groups (each containing two biological and two technical replicates) for the analysis. The union of the modulated genes was assumed to be affected by the treatment.

Real-time polymerase chain reaction

Quantitative real-time polymerase chain reaction (RT-PCR) was performed to quantitate messenger RNA levels of a selection of genes in order to verify expression changes from the microarray experiments. Reverse transcription reaction was performed using 1 μg of total RNA using iScript cDNA Synthesis Kit (Bio-Rad Laboratories, Hercules, CA). Subsequently, RT-PCR reactions were performed using iQ™ SYBR® Green Supermix, containing iTaq DNA Polymerase, deoxynucleoside triphosphates and SYBR Green I (Bio-Rad Laboratories). All PCR reactions were performed in duplicate. β-actin messenger RNA was used as reference in order to normalize expression levels and to quantitate changes in gene expressions between the control and treated samples. The RT-PCR was run on the MyiQ Single-Color Real-Time PCR Detection System (Bio-Rad Laboratories): 3 min at 95°C, 40 cycles of 95°C for 15 s and 60°C for 45 s. The following forward and reverse primers were used (OPERON, 5′-3′ sequences): *CYP1A1* TCCTGGAGACCTTCCGACACT (forward) and CTTTCAAACTTGTGTCTCTTGTTGTG (reverse), *GADD45A* CGACCTGCAGTTTGCAATATGA (forward) and CCCCCACCTTATCCATCCTT (reverse), *APOC3* GAAAGACTACTGGAGCACCGTTAAG (forward) and CACGGCTGAAGTTGGTCTGA (reverse), *HIF1A* TTTACCATGCCCCAGATTCAG (forward) and GGACTATTAGGCTCAGGTGAACTTTG (reverse) and *β-actin* CCTGGCACCCAGCACAAT (forward) and GCCGATCCACACGGAGTACT (reverse). Dissociation curve analysis was performed and 'no template controls' were analyzed to check for non-specific products in the reaction. For each sample, the quantity was derived from Ct = Ct(target gene)−Ct(β-actin reference). These values were log 2 transformed, and the difference of each test relative to their concomitant vehicle control sample was calculated (18).

Assessing additivity for gene expression modulation

Assuming additivity of both compounds in a mixture, the expected effects for a mixture can be calculated. Comparing the observed modulations with the

expected may provide information on whether the effects caused by mixtures are additive, synergistic or antagonistic.

To calculate the expected gene expression modulation by a mixture of two compounds based on the modulations of the individual compounds, only genes were included which were significantly modulated by either of the individual compounds or the mixture and which had the same direction of modulation (up or down). Genes of which the expression difference (log transformed) was between −0.1 and 0.1 were assumed to be similarly regulated as the other compound of the mixture.

For up-regulated genes, starting with ^{2}log transformed expression ratios of the individual PAHs, the next formulae, were used to calculate the expected ^{2}log transformed expression ratio for a gene in the mixture:

$$2^{2\log(\mathrm{PAH}/C)} = (PAH/C).$$

In which PAH is the expression of a gene following treatment with a PAH and C is the expression of a gene following control treatment (DMSO). In this step, the ^{2}log transformed expression ratios are transformed back into non-logarithmic values.

$$\frac{\text{Mixture}}{C} = (\mathrm{B}[a]\mathrm{P}/C) + (\mathrm{PAH}/C) - 1.$$

The expected effect of the mixture B[a]P and a PAH equals the sum of the effect of B[a]P and of the other PAH minus the basal gene expression level of 1.

$$\text{The expected } {}^2\text{log transformed expression ratio for a gene in a mixture:} = {}^2\log((\mathrm{B}[a]\mathrm{P}/C)+(\mathrm{PAH}/C) - 1).$$

For down-regulated genes, starting with ^{2}log transformed expression ratios of the individual PAHs, the following formulae were used to calculate the expected ^{2}log transformed expression ratio for a gene in a mixture:

$$1/2^{2\log(\mathrm{PAH}/C)} = (C/\mathrm{PAH}).$$

In which PAH is the expression of a gene following treatment with a PAH and C is the expression of a gene following control treatment (DMSO). In this step, the ^{2}log transformed expression ratios are transformed back into non-logarithmic values, followed by a calculation of its inverse (hereby the effects are transformed into up-regulations). Then the same procedure is followed as above (from step 2 onwards), finalized with inversing back the value before log transformation.

Finally, the observed gene expression values (y-axis) were plotted versus the expected values (x-axis). Linear regression analysis and Pearson correlation coefficients were calculated using SPSS 12.0.1 for windows (SPSS, Chicago, IL). Additivity was assumed when regression analysis for the observed and expected data did not show a deviation from $y = x$ (confidence interval of 2 SD). If it did deviate from $y = x$, synergism is shown by a slope >1 and antagonism by a slope <1.

To assess whether the expression of single genes showed additivity, the formulae as described above were used. Expected gene expression levels showed additive response if they fall within the confidence interval (1 SD) of the observed gene expression modulation. If not, the gene was classified as being higher or lower expressed than expected for that mixture.

Results

Equimolar concentrations

Apoptosis and cell cycle changes Flow cytometric analysis of cells exposed to B[a]P, DB[a,l]P or an equimolar mixture of both compounds showed dose-dependent induction of apoptosis (supplementary Figure 1 is available at Carcinogenesis Online). DB[a,l]P and the mixture increased apoptosis levels from 0.1 μM and higher, whereas for B[a]P this was at 3 μM and higher.

An increase of cells in S-phase was seen after 0.01 μM with a subsequent decrease from 0.1 μM for all treatments (Figure 1). For B[a]P, an increased percentage of cells in S-phase was observed from 0.3 μM and higher, and DB[a,l]P and the mixture showed increased S-phase from 0.01 to 0.003 μM and higher, respectively.

Based on these data, concentrations of 0.1, 0.3 and 1.0 μM were used for gene expression analysis.

Gene expression modulation Microarray analysis showed that a total number of 127 genes were affected by one or more treatments. For B[a]P 2, 5 and 6 genes were modulated by, respectively, 0.1, 0.3 and 1.0 μM exposure, for DB[a,l]P 7, 29 and 72 genes were affected and for the mixture 6, 49 and 77 genes. Many, but not all, genes affected by B[a]P or DB[a,l]P were also affected by the mixture, although the mixture also affected genes which were not modulated by one of the constituents. Names, abbreviations, GenBank accession numbers and gene expression differences of the modulated genes can be found in the supplementary data file (Table 2 is available at Carcinogenesis Online).

Principal component analysis, Figure 2, showed that gene expression profiles induced by B[a]P are similar for all concentrations and different from either the mixture or DB[a,l]P. The gene expression profiles of DB[a,l]P and the mixture treatments were closely related between each concentration of treatment, but the resemblance between gene expression profiles induced by DB[a,l]P and the mixture decreased with increasing concentration of treatment. This suggests a contribution of B[a]P to the mixture at the higher concentrations.

Assessing the additivity of effects induced by the mixture By using the gene expression profiles of B[a]P and DB[a,l]P, it was possible to calculate the expected effect of the mixture for the significantly modulated genes. Expected gene expression levels were plotted against observed expression levels for all concentrations (Figure 3). For the 0.3 and 1.0 μM treatments, the correlation coefficient was significant ($P < 0.05$). At 1.0 μM, we found a significant deviation from the line

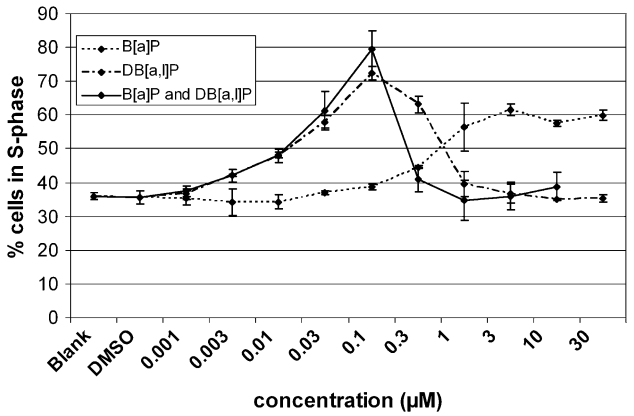

Fig. 1. Percentage of HepG2 cells in the S-phase of cell cycle after exposure to B[a]P, DB[a,l]P or their equimolar mixture for 24 h. Means of duplicate experiments and their standard deviation are indicated.

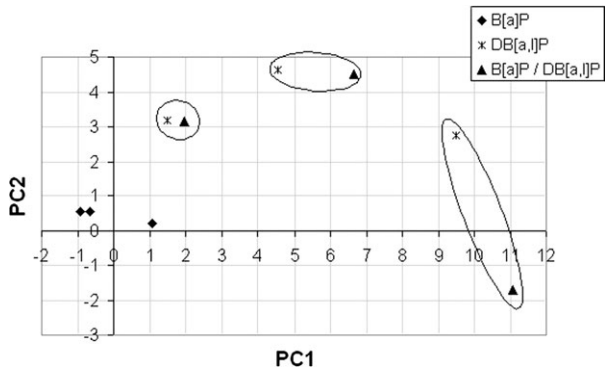

Fig. 2. Principal component analysis of gene expression differences in HepG2 cells after exposure for 24 h to B[a]P, DB[a,l]P or their equimolar mixture with the 127 genes differentially expressed by either of the treatments. Each circle contains the same concentration of treatment with DB[a,l]P and the mixture of B[a]P and DB[a,l]P.

$y = x$ in these regression models, where antagonism is shown (slope < 1). The mixture effects at 0.1 and 0.3 μM are unclear due to the small contribution of B[*a*]P to the mixture.

Also, individual genes show interactive effect after exposure to the mixture. The expression of 12 genes consistently showed additivity of the gene expression of the mixture. These genes were *ACTGP3*, *ATF3*, *CDH2*, *CDKN1A*, *CHK*, *CYP2C19*, *GADD45A*, *HAMP*, *MMP3*, *MT2A*, *SLC6A9* and an unknown gene with GenBank accession number XM_010682. No genes showed consistent antagonistic or synergistic responses.

Equitoxic concentrations

Apoptosis and cell cycle changes Apoptosis and cell cycle disturbances were measured for each of the six PAHs in concentrations ranging from 0.01 to 30 μM. All PAHs increased apoptosis levels in HepG2 cells, except FA and 1-MPA (supplementary Figure 2A, available at Carcinogenesis Online). B[*a*]P, DB[a,l]P, B[b]F and DB[a,h]A increased apoptosis levels from 3.0, 0.1, 10.0 and 1.0 μM and higher, respectively.

Many PAHs also increased the number of cells in S-phase; only FA and 1-MPA did not affect cell cycle (supplementary Figure 2B, available at Carcinogenesis Online). B[*a*]P, DB[a,l]P, B[b]F and DB[a,h]A disturbed cell cycle from 0.3, 0.01, 0.1 and 0.03 μM and higher, respectively.

Concentrations to study the effects of equitoxic concentrations were selected based on these apoptosis and cell cycle data. Each PAH affected both parameters at similar concentrations, only B[b]F disturbed cell cycle at much lower concentrations than apoptosis induction. As FA and 1-MPA did not change either apoptosis or in cell cycle, the highest concentration (30 μM) was used to study the effects of mixtures with B[*a*]P. The concentrations selected for B[*a*]P, DB[a,l]P, B[b]F and DB[a,h]A were, respectively, 3.0, 0.1, 3.0 and 1.0 μM.

None of the apoptosis levels induced by the mixture of a PAH with B[*a*]P differed significantly from the expected effect (Figure 4). The percentage of cells in S-phase of cell cycle after treatment with a mixture resembled mostly that after B[*a*]P treatment (no significant deviation; Figure 4).

DNA adduct formation DNA adduct formation as measured by ^{32}P-post-labelling in the HepG2 cells exposed to the equitoxic concentrations of PAHs is shown in Figure 5. DNA adduct formation for equitoxic concentrations was B[*a*]P > B[b]F > DB[a,l]P ≥ DB[a,h]A > FA ≥ 1-MPA. Interestingly, the mixtures of B[*a*]P with FA or 1-MPA induced the highest DNA adduct levels, whereas FA and 1-MPA itself did not induce DNA adducts. For these treatments, the B[*a*]P adduct spots were increased and no other adducts were found. All mixtures showed higher DNA adduct levels than expected, which indicates a synergistic effect on DNA adduct formation.

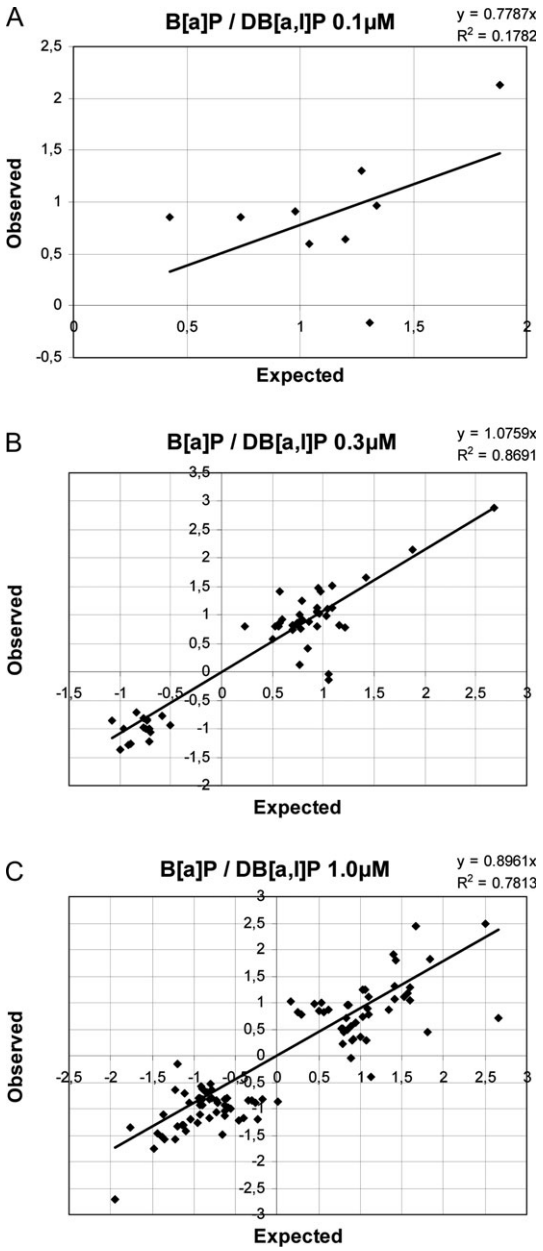

Fig. 3. Expected (based on additivity) versus observed gene expression of the equimolar mixture of B[*a*]P and DB[a,l]P for the concentrations 0.1, 0.3 and 1.0 μM in **a**, **b** and **c**, respectively. Correlation coefficients (R^2) and the line equation are indicated in the graph.

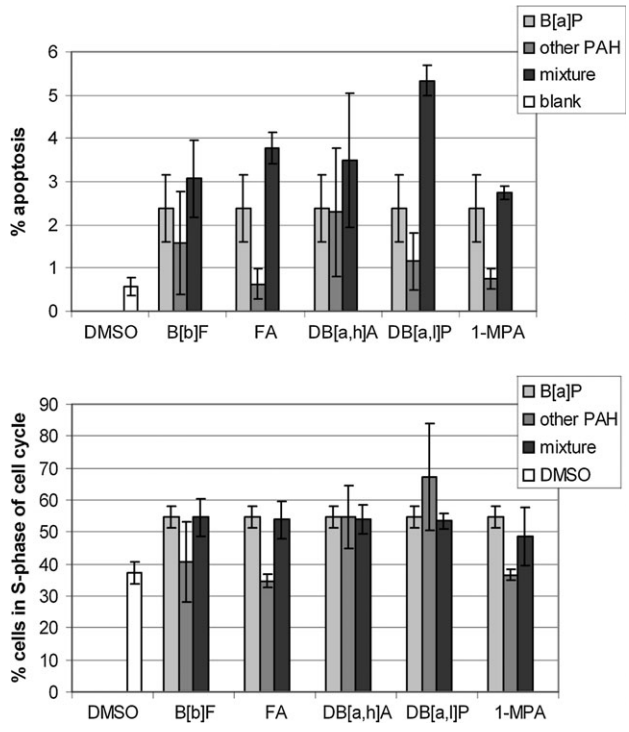

Fig. 4. Apoptosis in HepG2 cells (**a**) or percentage of HepG2 cells in the S-phase of cell cycle (**b**) after exposure to B[*a*]P, DB[a,l]P, DB[a,h]A, B[b]F, FA or 1-MPA or a mixture of each PAH with B[*a*]P for 24 h expressed as a percentage of total cells. Means of duplicate experiments and their standard deviation are indicated.

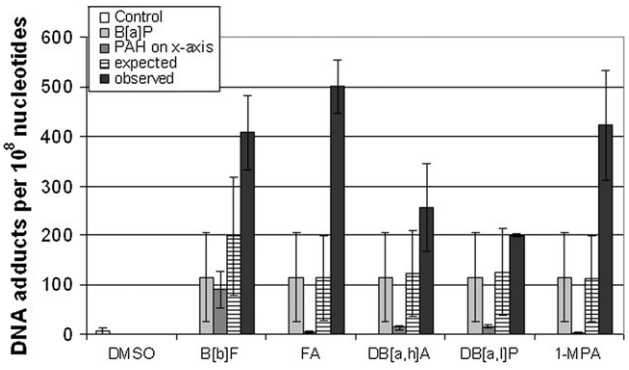

Fig. 5. DNA adduct formation in HepG2 cells exposed to equitoxic concentrations of PAHs for 24 h as measured by ^{32}P-post-labelling. The mean number of DNA adducts per 10^8 nucleotides and their standard deviations are shown. Expected is based on additivity of the constituents of the mixture.

Gene expression modulation In total, 54 genes were modulated by one or more treatments, varying from one gene for the 1-MPA and FA treatments to 37 genes by the treatment with a mixture of B[*a*]P/B[b]F. The numbers of modulated genes for each treatment and the overlap between treatments shows that most genes modulated by a single compound were also modulated by their mixture with B[*a*]P (supplementary Figure 3 is available at Carcinogenesis Online). Names, abbreviations, GenBank accession numbers and gene expression differences of the modulated genes can be found in the supplementary data (Table 3 is available at Carcinogenesis Online).

Assessing the additivity of effects induced by the mixture Expected gene expression profiles of the mixture were calculated based on the gene expression profiles of its individual compounds and plotted against the observed expression levels (Figure 6). All correlation coefficients were significant. Regression analysis showed that only mixtures with DB[a,l]P and 1-MPA deviate significantly from the line $y = x$, and the observed values were smaller than expected (slope <1), indicating an antagonistic effect. For mixtures of B[*a*]P with either B[b]F, DB[a,h]A or FA this deviation was not observed, suggesting an additive effect for these mixtures.

Comparing the observed and expected gene expression level for single genes showed that for 14 genes the observed and expected values did not differ of the gene expression of the mixture. Also, we found a synergistic or antagonistic effect on gene expression for 12 out of 55 modulated genes (observed consistently higher or lower than expected). Table I shows the interactive effects of each gene for all mixtures. An overview of all interactive effects in equitoxic mixtures is shown in Table II.

Validation by RT-PCR Gene expression modulation and interactive effects for four genes (*CYP1A1*, *GADD45A*, *APOC3* and *HIF1A*) was validated by quantitative RT-PCR. The direction of modulation was similar for all genes assessed and each of the treatments (single compounds and mixtures), although the extent of modulation was slightly higher for RT-PCR compared with microarray analysis (supplementary Figure 4 is available at Carcinogenesis Online). For each gene and mixture, the interactive effect is similar for microarray analysis and RT-PCR, as shown in Figure 7. This indicates that the interactive results obtained by microarray analysis are an accurate estimation of the interactive effect of PAH mixtures on gene expression.

Discussion

This study focuses on the effects of binary mixtures of PAHs on cell cycle, apoptosis, DNA adduct formation and gene expression modulation. We compared the observed gene expression effects of equimolar and equitoxic PAH mixtures with the expected data based on additivity of its individual compounds in HepG2 cells. We aim to gain insight into the effects of PAH mixtures and test possibility synergistic, antagonistic or additive effects of a mixture. Mixtures were assessed on their interactive effects based on an additive model. Deviation from this model indicated either synergism or antagonism.

Cell cycle and apoptosis

The effect on cell cycle and apoptosis in HepG2 cells treated with equimolar concentrations of B[*a*]P and DB[a,l]P was found to resemble the effects of DB[a,l]P alone. B[*a*]P had little effect on apoptosis and therefore did not contribute to the apoptosis of HepG2 cells exposed to the B[*a*]P/DB[a,l]P mixture. B[*a*]P did block cells in S-phase of cell cycle, although at higher concentrations than DB[a,l]P and therefore the effect of B[*a*]P on cell cycle in the equimolar B[*a*]P/DB[a,l]P mixture mainly represented the effects of DB[a,l]P.

Of all six PAHs tested, we found that DB[a,l]P and B[*a*]P are most toxic to HepG2 cells in the concentration range tested. Effects on cell cycle were shown by an increased number of cells in S-phase, which has been observed in other studies as well (19).

Equitoxic mixtures of each PAH with B[*a*]P showed slightly increased levels of apoptosis compared with the compounds individually. Only FA and DB[a,l]P showed some synergism. Interaction on S-phase arrest did not occur. No comparable literature data were available.

DNA adduct formation

DNA adduct formation in HepG2 cells after exposure to equitoxic PAH concentrations showed that equally toxic concentrations (based on apoptosis and cell cycle disturbances) did not induce the same level of DNA adducts in HepG2 cells. This indicates that the cytotoxic effects are not directly related to the total DNA adduct levels. Mixtures of two PAHs showed synergism on DNA adducts formation for all mixtures. Possibly, PAH activation is enhanced in co-exposure of PAHs leading to a higher level of DNA reactive metabolites. This seems to be indicated by a synergistic effect on the expression of *CYP1A2* which we found for B[*a*]P/DB[a,h]A and B[*a*]P/DB[a,l]P. Or, as Uno *et al.* (2) found increased levels of DNA adducts in *CYP1A1* knockout mice, which results in a reduced metabolism of PAHs in mixtures, and may lead to higher DNA adduct levels. Also, phase II enzymes involved in detoxifying PAH metabolites might be saturated and thereby leading to increased levels of PAH metabolites.

Our findings were not supported by earlier studies, in which an antagonistic effect of PAH mixtures on DNA adduct formation was found in MCF7 cells (20), which may be due to the differences between breast tissue and actively metabolizing liver tissue or to the more complex mixtures studied. The synergistic effect found on DNA adduct formation seems to be strongest for FA and 1-MPA, which did not induce DNA adducts individually, but which are neither inducers of CYP450 activity. This might prove an important role of these low carcinogenic compounds in co-carcinogenesis, though the mechanism is currently not understood.

Gene expression modulation

For DB[a,l]P, FA and 1-MPA low numbers of genes were found to be affected in the equitoxic experiment. As we used the highest dose of 30 μM for the latter two compounds, these compounds probably have little effect on gene expression in HepG2 cells, as was shown previously (7). For DB[a,l]P, we used the 0.01 μM concentration since at this dose it already showed increased apoptosis levels and marked cell cycle changes. However, DB[a,l]P had a small effect on gene expression at this concentration.

Assessing the additivity of gene expression profiles for mixtures

As the effects in equimolar mixtures were dominated by the effects of DB[a,l]P, we did not include those data in assessing the interactive effects of PAH mixtures. However, the effects at the highest concentration,

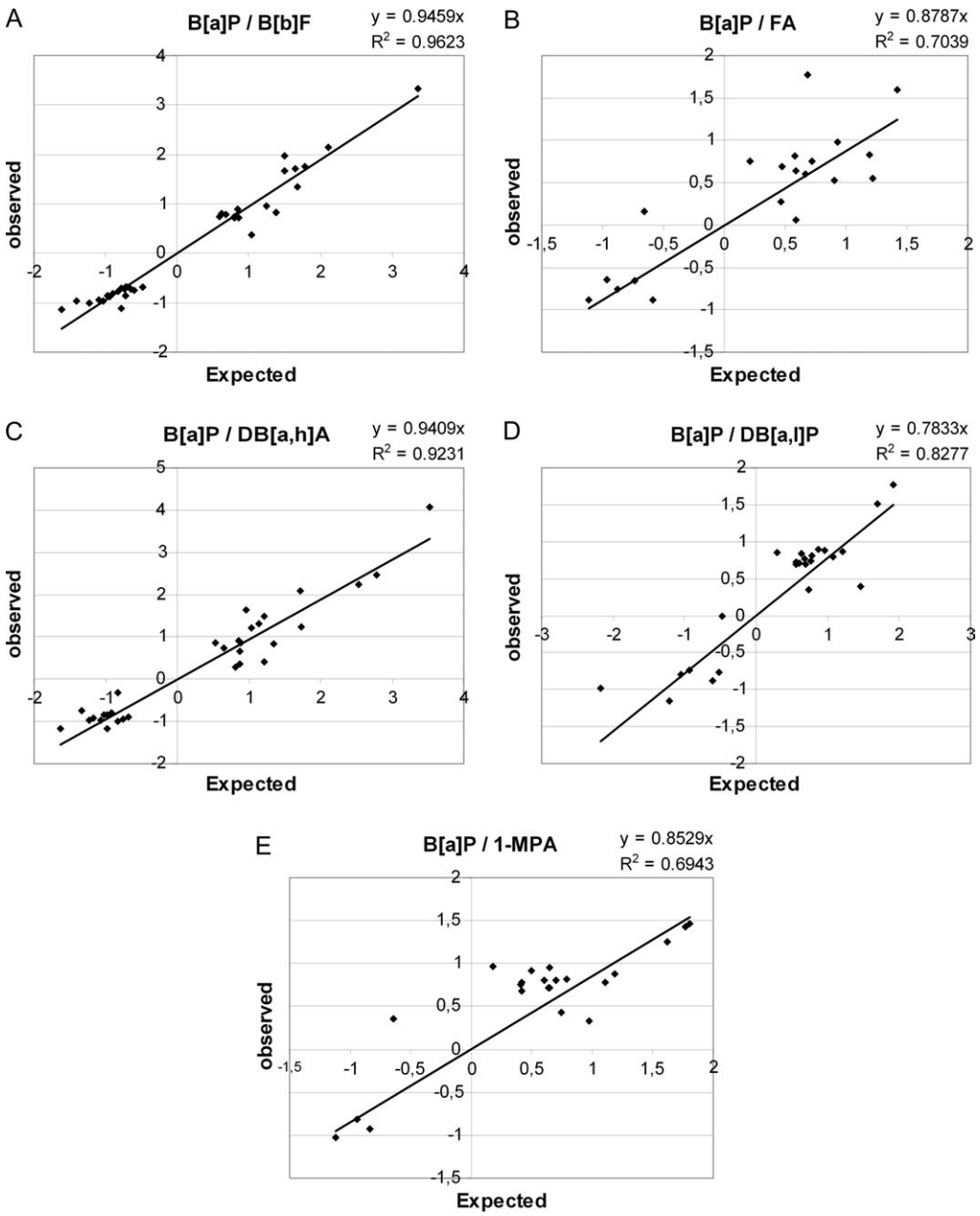

Fig. 6. Expected (based on additivity) (*x*-axis) versus observed (*y*-axis) gene expression of the equitoxic mixture of B[*a*]P and B[b]F (**a**), FA (**b**), DB[a,h]A (**c**), DB[a,l]P (**d**) or 1-MPA (**e**). Correlation coefficients (R^2) and the line equation are indicated in the graph.

at which both compounds contributed to the effects of the mixture, shows antagonism, which agrees with the effects shown by this mixture at equitoxic concentrations. However, only eight genes were significantly modulated at the highest concentration of the equimolar mixture and by the equitoxic mixture of B[*a*]P/DB[a,l]P.

Comparison of observed and expected gene expression levels (Figure 6) showed that the interactive effects on gene expression profiles differ between PAH mixtures. Mixtures of B[*a*]P with B[b]F, FA and DB[a,h]A showed additive effects on gene expression, whereas the mixtures of B[*a*]P with DB[a,l]P and with 1-MPA showed antagonism.

Assessing additivity of differential expression for single genes

The expression of many genes showed additivity for many conditions in either of the experiments. Some of these genes are involved in PAH metabolism, like *CYP1A1*, and many others are related to tumorigenesis. Only one gene was found to show additivity at the equimolar as well as the equitoxic concentrations, which was *ATF3*. Since only one gene shows similar interaction in the equimolar and equitoxic mixtures, it shows that interactive effects are dependent on the concentrations selected.

Furthermore, 13 genes showed mostly synergism or antagonism in the various mixtures (Table I). Many of these genes can be related to DNA damage induces by PAH and the early onset of carcinogenesis. These genes include *XRCC1* and *GADD45a*, which are involved in DNA damage repair (21,22), and *MT2A* which is involved in protection against oxidative stress (23). The expression of many of these carcinogenesis-related genes is higher expressed than expected, indicating a higher damaging effect of PAHs in mixtures than the individual compounds suggest. This is in agreement with the levels of DNA adducts we found after exposure to PAH mixtures. The expression of some other genes related to cell cycle or DNA damage (CDKN1A and BAX) did not show interaction for more than one mixture.

Table I. Interactive effect on gene expression upon exposure to equitoxic PAH mixtures

Genbank accession	GeneSymbol	GeneName	B[*a*]P + 1-MPA	B[*a*]P + B[b]F	B[*a*]P + DB[a,h]A	B[*a*]P + DB[a,l]P	B[*a*]P + FA
Additivity							
L19871	*ATF3*	Activating transcription factor 3		=	=		
XM_005207	*CA3*	Carbonic anhydrase III, muscle specific		=	=	=	
L08599	*CDH1*	Cadherin 1, type 1, E-cadherin (epithelial)		=			=
M18728	*CEACAM6*	Carcinoembryonic antigen-related cell adhesion molecule 6 (non-specific cross reacting antigen)	=			=	
K03191	*CYP1A1*	Cytochrome P450, family 1, subfamily A, polypeptide 1	=	=	=		
NM_004104	*FASN*	Fatty acid synthase		=	=		
X51473	*FGG*	Fibrinogen, gamma polypeptide		=	=		
L37080	*FMO5*	Flavin-containing monooxygenase 5		=	=		
M37484	*IGF1*	Insulin-like growth factor 1 (somatomedin C)	=	=	=	=	=
M31145	*IGFBP1*	Insulin-like growth factor-binding protein 1	=	=	=	=	
08246	*MCL1*	Myeloid cell leukemia sequence 1 (BCL2-related)	=	=	=		
M55580	*SAT*	Spermidine/spermine N1-acetyltransferase	=	=	=	=	=
AB032261	*SCD*	Stearoyl-CoA desaturase (delta-9-desaturase)		=	=		
NM_003332	*TYROBP*	TYRO protein tyrosine kinase-binding protein			=	=	=
XM_005563			=	=	=	=	=
Mostly synergism							
J05474	*AKR1B1*	Aldo-keto reductase family 1, member B1 (aldose reductase)		=	+		+
XM_003872	*AMACR*	Alpha-methylacyl-CoA racemase	+		=	+	
NM_000761	*CYP1A2*	Cytochrome P450, family 1, subfamily A, polypeptide 2		=	+	+	
M10617	*FABP1*	Fatty acid-binding protein 1, liver		+	=	=	+
M60974	*GADD45A*	Growth arrest and DNA-damage-inducible, alpha	+	+		=	
X97260	*MT1E*	Metallothionein 1E (functional)	+	=	=	+	
M36089	*XRCC1*	X-ray repair complementing defective repair in Chinese hamster cells 1	+				+
Mostly antagonism							
X03120	*APOC3*	Apolipoprotein C-III	=	−	−	=	−
D49471	*ECE1*	Endothelin-converting enzyme 1	=	−	−	−	=
XM_004994	*GCK*	Glucokinase (hexokinase 4, maturity onset diabetes of the young 2)	=	−	−	−	−
U22431	*HIF1A*	Hypoxia-inducible factor 1, alpha subunit (basic helix-loop-helix transcription factor)	−	=	−	−	=
K01500	*SERPINA3*	Serine (or cysteine) proteinase inhibitor, clade A (alpha-1 antiproteinase, antitrypsin), member 3	−	−	=	=	−
J04765	*SPP1*	Secreted phosphoprotein 1 (osteopontin, bone sialoprotein I, early T-lymphocyte activation 1)	−	−	−		−
Other interactions							
M11313	*A2M*	Alpha-2-macroglobulin	−		=	=	=
J05474	*AKR1B1*	Aldo-keto reductase family 1, member B1 (aldose reductase)		=			
L22473	*BAX*	BCL2-associated X protein					+
U03106	*CDKN1A*	Cyclin-dependent kinase inhibitor 1A (p21, Cip1)	+			=	=
M17303	*CEACAM5*	Carcinoembryonic antigen-related cell adhesion molecule 5	+			=	
AB017493	*COPEB*	Core promoter element-binding protein	+				
M13699	*CP*	Ceruloplasmin (ferroxidase)					=
M29874	*CYP2B6*	Cytochrome P450, family 2, subfamily B, polypeptide 6			+		
M58569	*FGA*	Fibrinogen, A alpha polypeptide		=	=		
M64082	*FMO1*	Flavin-containing monooxygenase 1					
X03674	*G6PD*	Glucose-6-phosphate dehydrogenase	=	=	=	−	=
XM_004453	*HIST1H2AL*	Histone 1, H2al		=			
XM_004419	*HIST1H3D*	Histone 1, H3d		=			
M11058	*HMGCR*	3-hydroxy-3-methylglutaryl-coenzyme A reductase		=	=		
X15183	*HSPCA*	Heat shock 90 kDa protein 1, alpha		=			
M29645	*IGF2*	Insulin-like growth factor 2 (somatomedin A)		=	−		
M13577	*MBP*	Myelin basic protein					
U33199	*MDM2*	Mdm2, transformed 3T3 cell double minute 2, p53-binding protein (mouse)					=
X92720	*PCK2*	Phosphoenolpyruvate carboxykinase 2 (mitochondrial)		=			
J04718	*PCNA*	Proliferating cell nuclear antigen				+	
J04605	*PEPD*	Peptidase D		=			
AJ001417	*SLC22A3*	Solute carrier family 22 (extraneuronal monoamine transporter), member 3		=			

Table I. *Continued*

Genbank accession	GeneSymbol	GeneName	B[*a*]P + 1-MPA	B[*a*]P + B[b]F	B[*a*]P + DB[a,h]A	B[*a*]P + DB[a,l]P	B[*a*]P + FA
M12530	*TF*	Transferrin		=		+	
X79929	*TNFSF4*	Tumor necrosis factor (ligand) superfamily, member 4 (tax-transcriptionally activated glycoprotein 1, 34 kDa)		−			
M76125	*UBE2A*	Ubiquitin-conjugating enzyme E2A (RAD6 homolog)			=	+	
NM_030938	*VMP1*	Likely ortholog of rat vacuole membrane protein 1		=			

Additivity is shown by '=', synergism by '+' and antagonism by '−'.
In order to judge the type of interactions on gene expression, the effects caused by the two PAHs is added (expected change) and compared with the expression of that gene in response to mixture treatment (observed change). Similar expression results in additive response, a higher than expected change results in a synergistic response and a lower than expected change in an antagonistic response. See Materials and methods for a detailed explanation.

Table II. Summary of data comparison between observed and expected data for the equitoxic experiment

	Apoptosis	Cell cycle	DNA adduct formation	Gene expression	*CYP1A1* expression
B[*a*]P/B[b]F	Additive	Unclear	Synergism	Additive	Additive
B[*a*]P/FA	Additive/synergism	Unclear	Synergism	Additive	Unclear
B[*a*]P/DB[a,h]A	Additive	Unclear	Synergism	Additive	Additive
B[*a*]P/DB[a,l]P	Additive/synergism	Unclear	Synergism	Antagonism	Unclear
B[*a*]P/1-MPA	Additive	Unclear	Synergism	Antagonism	Additive

Additive effects have no difference between observed and expected data, for synergism the observed effect is higher than expected and for antagonism the observed effect is lower than expected.

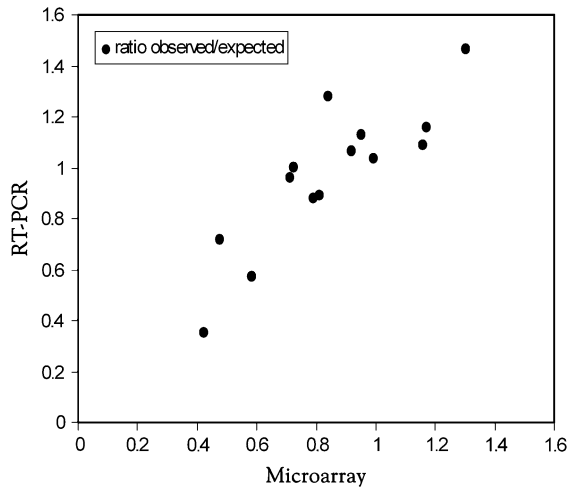

Fig. 7. Ratio between observed and expected gene expression changes for CYP1A1, GADD45A, APOC3 and HIF1A upon exposure to PAH mixtures based on microarray data and RT-PCR data.

Synergism or antagonism?

To our knowledge, no previous studies have been done on the interactive effects of mixtures on gene expression level. Therefore, we attempted to develop a method for assessing these effects. Although we realize this method may not be perfect, we have tried to design a method which allows studying effects of mixtures on gene expression level.

To assess the effects of PAH mixtures, an addition of concentrations is not always accurate (24), since a common mode of action is assumed. Alternatively, a model that assumes no common mode of action was found to predict the effects of the mixture more accurately. Our method adds effects on gene expression, and no common mode of action is required and therefore our method might be a good estimation of the effects of a mixture. However, further development is required, but our method could be useful for other researchers interested in interactive effects on gene expression level.

A comparison of interactive effects (Table II) shows that no consistent effects are observed for each mixture. Most previous studies suggest an additive effect or an antagonistic effect of PAH mixtures (4,25). This agrees with the effects we found on gene expression, which were also additive or antagonistic. Interactions of B[b]F, FA and DB[a,h]A with B[*a*]P on gene expression are mostly additive. On DNA adduct formation, the effects are all synergistic, however, and thus do not agree with the antagonistic or additive effects on gene expression or other parameters. We have no ready explanation for this difference. It might be related to the synergistic effect of PAH mixtures (B[*a*]P/DB[a,l]P and B[*a*]P/DB[a,h]A) on the expression of *CYP1A2*, which might result in increased formation of carcinogenic metabolites and thereby increased DNA adduct formation. The synergism we found for DNA adduct formation was not found by Gray *et al.* (26) for mixtures of B[*a*]P and 7H-dibenzo[c,g]carbazole on tumor formation in mice. This might be due to the different compounds tested or the difference of *in vivo* versus *in vitro*. However, James *et al.* (27) did find a synergism in toxicity of PAHs and Polychlorinated Biphenyls, which are also metabolized by the same enzymes of the cytochrome P450 family.

Although 1-MPA and FA did show some effect on the parameters tested individually, in mixtures both compounds showed to contribute to the effect of the mixture. This shows that compounds having little effect by itself, may contribute importantly to the effects of a mixture.

Furthermore, whereas the effects of B[*a*]P/DB[a,l]P and B[*a*]P/1-MPA on gene expression can be antagonistic, the effects on other parameters can show synergism. Uno *et al.* (2) found that levels of DNA adducts were higher in *CYP1A1* knockout mice. So, by its antagonistic effect on gene expression (including *CYP1A1*), of both mixtures, the levels of DNA adducts may be increasing, which is in accordance with what we found.

Conclusion

In our study, we showed that many PAH mixtures show mostly additive or antagonistic effects on gene expression profiles, apoptosis and

cell cycle. For individual genes, the expression of a few genes showed additivity, but many genes showed interactive effects. The only consistent interactive effect was on DNA adduct formation, which was always synergistic. Also, compounds like FA and 1-MPA, which do not induce adducts and are weak or not carcinogenic, have an impact on the effects of mixtures and thus affect the carcinogenic potency of PAH mixtures. The synergistic effects of PAH mixtures on DNA adduct formation suggest a higher carcinogenic potency of PAHs than based on the individual compounds. However, as the effects on gene expression are in opposite direction, it cannot be firmly stated whether PAH mixtures have increased or decreased carcinogenic potencies.

Supplementary material

Supplementary Tables 1–3 and Figures 1–4 can be found at http://carcin.oxfordjournals.org/

Funding

European Union (QRLT-2001-024202).

Acknowledgements

The research was carried out as part of the AMBIPAH project (mechanism-based approaches to improve cancer risk assessment of ambient air polycyclic aromatic hydrocarbons).

Conflict of Interest Statement: None declared.

References

1. Shimada,T. *et al*. (2003) Tissue-specific induction of cytochromes P450 1A1 and 1B1 by polycyclic aromatic hydrocarbons and polychlorinated biphenyls in engineered C57BL/6J mice of arylhydrocarbon receptor gene. *Toxicol. Appl. Pharmacol.*, **187**, 1–10.
2. Uno,S. *et al*. (2006) Oral benzo[a]pyrene in Cyp1 knockout mouse lines: CYP1A1 important in detoxication, CYP1B1 metabolism required for immune damage independent of total-body burden and clearance rate. *Mol. Pharmacol.*, **69**, 1103–1114.
3. Shimada,T. *et al*. (2002) Arylhydrocarbon receptor-dependent induction of liver and lung cytochromes P450 1A1, 1A2, and 1B1 by polycyclic aromatic hydrocarbons and polychlorinated biphenyls in genetically engineered C57BL/6J mice. *Carcinogenesis*, **23**, 1199–1207.
4. Nesnow,S. *et al*. (1998) Lung tumorigenic interactions in strain A/J mice of five environmental polycyclic aromatic hydrocarbons. *Environ. Health. Perspect.*, **106** (suppl. 6), 1337–1346.
5. Ross,J.A. *et al*. (1995) Adenomas induced by polycyclic aromatic hydrocarbons in strain A/J mouse lung correlate with time-integrated DNA adduct levels. *Cancer Res.*, **55**, 1039–1044.
6. Solhaug,A. *et al*. (2004) Polycyclic aromatic hydrocarbons induce both apoptotic and anti-apoptotic signals in Hepa1c1c7 cells. *Carcinogenesis*, **25**, 809–819.
7. Staal,Y.C. *et al*. (2006) Modulation of gene expression and DNA adduct formation in HepG2 cells by polycyclic aromatic hydrocarbons with different carcinogenic potencies. *Carcinogenesis*, **27**, 646–655.
8. Cassee,F.R. *et al*. (1998) Toxicological evaluation and risk assessment of chemical mixtures. *Crit. Rev. Toxicol.*, **28**, 73–101.
9. Freedman,M.D. (1995) Drug interactions: classification and systematic approach. *Am. J .Ther.*, **2**, 433–443.
10. Liebler,D.C. (1993) The role of metabolism in the antioxidant function of vitamin E. *Crit. Rev. Toxicol.*, **23**, 147–169.
11. Cherng,S.H. *et al*. (2006) Suppressive effect of 1-nitropyrene on benzo[a]-pyrene-induced CYP1A1 protein expression in HepG2 cells. *Toxicol. Lett.*, **161**, 236–243.
12. Willett,K.L. *et al*. (2001) In vivo and in vitro inhibition of CYP1A-dependent activity in Fundulus heteroclitus by the polynuclear aromatic hydrocarbon fluoranthene. *Toxicol. Appl. Pharmacol.*, **177**, 264–271.
13. IARC. (1973) Certain polycyclic aromatic hydrocarbons and heterocyclic compounds. *IARC Monogr. Eval. Carcinog. Risk Chem. Hum.*, **3**, 1–271.
14. IARC. (1983) Polynuclear aromatic compounds, Part 1, Chemical, environmental and experimental data. *IARC Monogr. Eval. Carcinog. Risk Chem. Hum.*, **32**, 1–453.
15. Reddy,M.V. *et al*. (1986) Nuclease P1-mediated enhancement of sensitivity of 32P-postlabeling test for structurally diverse DNA adducts. *Carcinogenesis*, **7**, 1543–1551.
16. Godschalk,R.W. *et al*. (1998) Differences in aromatic-DNA adduct levels between alveolar macrophages and subpopulations of white blood cells from smokers. *Carcinogenesis*, **19**, 819–825.
17. Staal,Y.C. *et al*. (2005) Application of four dyes in gene expression analyses by microarrays. *BMC Genomics*, **6**, 101.
18. Livak,K.J. *et al*. (2001) Analysis of relative gene expression data using real-time quantitative PCR and the 2(-Delta Delta C(T)) method. *Methods*, **25**, 402–408.
19. Binkova,B. *et al*. (2000) The effect of dibenzo[a,l]pyrene and benzo[a]pyrene on human diploid lung fibroblasts: the induction of DNA adducts, expression of p53 and p21(WAF1) proteins and cell cycle distribution. *Mutat. Res.*, **471**, 57–70.
20. Mahadevan,B. *et al*. (2004) Effect of artificial mixtures of environmental polycyclic aromatic hydrocarbons present in coal tar, urban dust, and diesel exhaust particulates on MCF-7 cells in culture. *Environ. Mol. Mutagen.*, **44**, 99–107.
21. Caldecott,K.W. *et al*. (1994) An interaction between the mammalian DNA repair protein XRCC1 and DNA ligase III. *Mol. Cell. Biol.*, **14**, 68–76.
22. Vairapandi,M. *et al*. (2002) GADD45b and GADD45g are cdc2/cyclinB1 kinase inhibitors with a role in S and G2/M cell cycle checkpoints induced by genotoxic stress. *J. Cell. Physiol.*, **192**, 327–338.
23. Reinecke,F. *et al*. (2006) Metallothionein isoform 2A expression is inducible and protects against ROS-mediated cell death in rotenone-treated HeLa cells. *Biochem. J.*, **395**, 405–415.
24. Olmstead,A.W. *et al*. (2005) Joint action of polycyclic aromatic hydrocarbons: predictive modeling of sublethal toxicity. *Aquat. Toxicol.*, **75**, 253–262.
25. Falahatpisheh,M.H. *et al*. (2001) Antagonistic interactions among nephrotoxic polycyclic aromatic hydrocarbons. *J. Toxicol. Environ. Health A*, **62**, 543–560.
26. Gray,D.L. *et al*. (2001) The effects of a binary mixture of benzo(a)pyrene and 7H-dibenzo(c,g)carbazole on lung tumors and K-ras oncogene mutations in strain A/J mice. *Exp. Lung. Res.*, **27**, 245–253.
27. James,M.O. *et al*. (2004) Increased toxicity of benzo(a)pyrene-7,8-dihydrodiol in the presence of polychlorobiphenylols. *Mar. Environ. Res.*, **58**, 343–346.

Received January 9, 2007; revised August 2, 2007; accepted August 2, 2007